

**INTERCONNECT CROSSTALK MINIMIZATION:
AN ALTERNATIVE ROUTE**

J.W. Bandler and J.E. Rayas-Sánchez

SOS-98-8-R
April 1998

© J.W. Bandler and J.E. Rayas-Sánchez 1998

No part of this document may be copied, translated, transcribed or entered in any form into any machine without written permission. Address inquiries in this regard to Dr. J.W. Bandler. Excerpts may be quoted for scholarly purposes with full acknowledgment of source. This document may not be lent or circulated without this title page and its original cover.

INTERCONNECT CROSSTALK MINIMIZATION: AN ALTERNATIVE ROUTE

J.W. Bandler and J.E. Rayas-Sánchez

Simulation Optimization Systems Research Laboratory
and Department of Electrical and Computer Engineering
McMaster University, Hamilton, Canada L8S 4L7

Tel 905 525 9140 Ext. 24305

Fax 905 523 4407

Email: rayassje@mcmaster.ca

Abstract An alternative approach to efficiently simulate and minimize the crosstalk between interconnects is presented in this report. Different ways to model the coupled microstrip transmission lines are discussed. Several possible simulation strategies are also considered. A straightforward frequency domain approach is proposed. A typical example of microstrip interconnects is simulated and the results are compared with previous work of other researchers. A crosstalk minimization problem is formulated and resolved following the method proposed.

I. INTRODUCTION

The performance of high speed electronic systems critically depends on the quality of the transmitted signals, that should be undisturbed, undistorted, and with the desired speed. As the general speed of operation of electronic circuits increases, more and more attention must be paid to the design of interconnects.

The crosstalk minimization problem associated to the design of interconnects has gained great importance for the following reasons:

- (a) the recent advances on integrated circuits technologies (GaAs MESFET, HEMT, etc.) has

This work was supported in part by the Natural Sciences and Engineering Research Council of Canada under Grants OGP0007239, OGP0042449 and STP0201832 and through the Micronet Network of Centres of Excellence. J.E. Rayas-Sánchez is funded by CONACYT (Consejo Nacional de Ciencia y Tecnología, Mexico), as well as by ITESO (Instituto Tecnológico y de Estudios Superiores de Occidente, Mexico).

- reduced the single device switching time to tens of picoseconds or less,
- (b) the development of VLSI circuit technologies and packaging techniques are yielding larger chips within smaller devices,
 - (c) the use of high density buses, at both the printed circuit board (PCB) and the multi-chip module (MCM) levels, has increased the proximity of interconnects.

When the physical length of interconnects becomes comparable to the wavelength of the highest frequency being transmitted, lumped impedance models can no longer be used for accurate simulation. Instead, a distributed transmission line model for the interconnect should be used. Further, the planar geometry used in integrated circuit technology allows that on-chip and inter-chip interconnections (PCBs, ASICs, ICs, MCMs) can be modeled as microstrip lines (Gao et al. [1]).

Much research has been accomplished on modeling and simulating microstrip lines as high speed interconnects. Most of the researchers have followed a time domain approach to simulate crosstalk between interconnects, measuring the transient waveform of the undesired signal. The weakness of this method is that crosstalk may vary extremely with frequency, so that the crosstalk simulated can increase very significantly with small changes in the transient input waveform. An alternative method to efficiently simulate and minimize the crosstalk between interconnects is proposed in this report, following a frequency domain approach.

II. CROSSTALK DEFINITION

The crosstalk between channels A and B is defined as the ratio of the output of channel A, with no signal input, divided by the output of channel B (see Fig. 1). In dB we measure crosstalk as

$$\text{Crosstalk} = 20 \log \left| \frac{V_{OA}}{V_{OB}} \right| \text{ dB} \quad (1)$$

Ideally, the crosstalk between channels that are supposed to be electrically unconnected should be zero. This is not the case when channels behave like coupled transmission lines.

III. COUPLED MICROSTRIP INTERCONNECTS

Fig. 2 illustrates the physical structure of a coupled microstrip interconnect, consisting of two horizontal flat conductors near a ground plane (FCNGP). Both conductors have the same length l and width w , and are mounted on a printed circuit wiring board with dielectric constant ϵ_r and thickness h . The conductors are separated a distance d . This physical representation is useful for PCB and MCM technologies.

The symbol shown in Fig. 3 will be used to represent the later coupled microstrip interconnect as a circuit component.

IV. MODELING THE INTERCONNECTS

Following Dhaene and De Zutter [2], the coupled lossless transmission line equations are

$$-\frac{d}{dz} \begin{bmatrix} \mathbf{V} \\ \mathbf{I} \end{bmatrix} = \begin{bmatrix} \mathbf{0} & \mathbf{Z} \\ \mathbf{Y} & \mathbf{0} \end{bmatrix} \begin{bmatrix} \mathbf{V} \\ \mathbf{I} \end{bmatrix} \quad (2)$$

where

$$\mathbf{V} = \begin{bmatrix} V_1 \\ V_2 \end{bmatrix} \quad \mathbf{I} = \begin{bmatrix} I_1 \\ I_2 \end{bmatrix} \quad (3)$$

are the voltages and currents along each line, and

$$\mathbf{Z} = j\omega\mathbf{L} = j\omega \begin{bmatrix} L_s & L_m \\ L_m & L_s \end{bmatrix} \quad \mathbf{Y} = j\omega\mathbf{C} = j\omega \begin{bmatrix} C_s & -C_m \\ -C_m & C_s \end{bmatrix} \quad (4)$$

are the self and mutual inductance (impedance) and capacitance (admittance) matrices.

It can be verified that a possible equivalent circuit is as illustrated in Fig. 4, where Δz represents a small increment along the transmission lines, so that the circuit components are distributed elements.

Several possible approaches have been followed to model the coupled microstrip interconnect.

A. Walker's model

Following Walker [3], the empirical formulas for the LC parameters of the above equivalent circuit are shown in Appendix A. The per-unit length LC parameters of coupled microstrip interconnects

obtained from Walker's formulas do not agree with those obtained by using an electromagnetic simulator (Bandler et al. [4]), which are more accurate. Walker's formulas can deviate from the corresponding values obtained by electromagnetic simulation by more than 50%.

B. SPICE model

According to Tripathi et al. [5], the coupled microstrip interconnect can be modeled by a circuit with two uncoupled transmission lines and eight polynomial controlled sources, as illustrated in Fig. 5. The L and C matrices and the length of the coupled microstrip interconnect can be used to obtain the circuit components, which are compatible with most CAD programs including SPICE.

A different SPICE model can be used by selecting an adequate number of elementary cells of the coupled lumped model (see Fig. 4), as recommended by Dhaene and De Zutter [2].

C. Frequency domain model (Kirschning-Jansen)

The Kirschning and Jansen frequency-domain model of the microstrip interconnect is based on expressions that have all been derived by successive computer matching to converged numerical results originated from a rigorous spectral-domain hybrid-mode approach. These analytical expressions describe the effective dielectric constants, the power-current characteristic impedances, and the equivalent open-end lengths of coupled microstrip lines (Kirschning and Jansen [6]). This model is accurate for the range of parameters

$$0.1 \leq \frac{w}{h} \leq 10 \quad (5a)$$

$$1 \leq \epsilon_r \leq 18 \quad (5b)$$

$$f(GHz) \leq \frac{30}{h(mm)} \quad (5c)$$

If the frequency domain model is used, it is necessary to employ the system voltage gain expression to derive the crosstalk information from the scattering parameters measured. The circuit shown in Fig. 6 shows a generic network characterized by its S parameters with respect to a reference

impedance Z_0 . It can be shown (Choma [7]) that the system voltage gain of the above general circuit is given by

$$A_V = \frac{V_O}{V_S} = \frac{S_{21}(1+\Gamma_l)(1-\Gamma_s)}{2[(1-S_{11}\Gamma_s)(1-S_{22}\Gamma_l)-S_{12}S_{21}\Gamma_l\Gamma_s]} \quad (6)$$

where

$$\Gamma_l = \frac{Z_L - Z_0}{Z_L + Z_0} \quad \text{and} \quad \Gamma_s = \frac{R_S - Z_0}{R_S + Z_0} \quad (7a,b)$$

are the reflection coefficients at the load and at the source, respectively.

In order to use simpler expressions, the network characterized by the S parameters can be conceptually expanded, as is illustrated in Fig. 7. That is, if $\Gamma_l = 1$ ($Z_L \rightarrow \infty$) and $\Gamma_s = -1$ ($R_S = 0$), then

$$A_V = \frac{V_O}{V_S} = \frac{2 S_{21}}{(1+S_{11})(1-S_{22})+S_{12}S_{21}} \quad (8)$$

V. SIMULATION OF A CROSSTALK PROBLEM

A. Problem definition

A classical problem that has been studied by several researchers is shown in Fig. 8. The circuit has three interconnects, several lumped passive components, one input signal, V_S , and four output voltages V_a , V_b , V_c and V_d . The simulator must be able to calculate the voltage at any output, as well as the crosstalk between any pair of outputs.

The lumped components values are as follows:

$$\begin{array}{lllll} R_1 = 50 \, \Omega & R_4 = 25 \, \Omega & R_7 = 100 \, \Omega & R_{10} = 100 \, \Omega & C_2 = 2 \, \text{pF} \\ R_2 = 75 \, \Omega & R_5 = 25 \, \Omega & R_8 = 100 \, \Omega & L = 10 \, \text{nH} & C_3 = 1 \, \text{pF} \\ R_3 = 100 \, \Omega & R_6 = 50 \, \Omega & R_9 = 50 \, \Omega & C_1 = 1 \, \text{pF} & \end{array}$$

In order to compare the simulation results with the corresponding ones obtained in previous work from other authors, the physical parameters were chosen as in [4] and [8], with the values $d = 2.49$ mm, h

= 1.17 mm, $w = 0.58$ mm, $\mu_r = 1$, $\epsilon_r = 5.182$, and the length of each interconnect as $L_1 = 5$ cm, $L_2 = 4$ cm, and $L_3 = 3$ cm. These values correspond to the following LC parameters obtained from Walker's formulas: $L_s = 494.5$ nH/m, $L_m = 63.29$ nH/m, $C_s = 69.97$ pF/m, $C_m = 7.94$ pF/m.

In this particular case, the Kirschning-Jansen frequency domain model of the interconnects should yield good accuracy for frequencies as high as 25.64 GHz (see equation 5c).

B. Simulation strategy

The simulation process, as well as the software tools to be used, inherently depends on the model chosen for the interconnect. The basic input data for any model of an interconnect are its physical parameters: h , ϵ_r , d , w . Once these parameters are determined, any of the following approaches could be followed.

A first approach could be realized by using Walker's formulas (see appendix A) to calculate the corresponding LC parameters and build up a SPICE model of the interconnect (i.e., Tripathi's model), and then use any circuit-level-time-domain SPICE compatible simulator, such as *Design Center*TM of Microsim [9].

A second approach can be developed by using an electromagnetic simulator to obtain the LC matrices, such as *em*TM [10] or *IE3D*TM [11], which can be then incorporated into the AWE simulator *COFFEE2* [12] developed at Carleton University.

An alternative approach may be accomplished by using the frequency domain characteristics of the interconnects and a frequency domain steady state CAD system *OSA90/hope*TM [13], which also offers powerful optimization capabilities.

All of the researchers reviewed (see References) have followed one of the first two approaches, since they measured the crosstalk effect in the time domain, transient response. The third approach was chosen in this work mainly because of four factors:

- (a) the accuracy of the Kirschning-Jansen frequency domain model of the interconnect, which is one of the built-in models available in *OSA90/hope*TM, is comparable with the one of the

electromagnetic simulators, within the frequency limitations of the model itself

- (b) the crosstalk phenomenon is of frequency domain nature, and can vary sharply within a given frequency range of operation, so it is crucial to measure it in the whole frequency range of operation
- (c) in spite of using the frequency domain model of the interconnect, the time domain steady state response of the circuit can be measured by using the harmonic balance simulation available in *OSA90/hope*TM
- (d) the minimization problem can be solved using the same CAD system, making the whole process straightforward

C. Frequency domain results

An *OSA90/hope*TM input file was designed for the frequency domain simulation of the circuit shown in Fig. 8, including (8) as AC postprocessing. The Kirschning-Jansen frequency domain model was employed using the built-in linear elements MSCL (two-conductor symmetrical coupled microstrip lines) and MSUB (microstrip substrate definition) directly available in *OSA90/hope*TM. Figs. 9 and 10 shows the crosstalk obtained between all circuit outputs.

The worst case, that is, the maximum crosstalk in the circuit, is the one between the output voltages V_a and V_b . As mentioned before, the crosstalk phenomenon varies significantly with the operating frequency, so that for any practical circuit, it is necessary to minimize the crosstalk to a certain specified value within the whole frequency range of interest.

D. Time domain results

An *OSA90/hope*TM input file was devised for the time domain simulation of the circuit shown in Fig. 8, using again the MSCL and MSUB linear built-in elements. The Harmonic Balance simulation technique is being used. As an input signal, the Fourier Exponential representation of the symmetrical trapezoid waveform of Fig. 11 was used (Sainati et al. [14]), given by:

$$V_S(t) = \sum_n a_n e^{+j\omega_n t} \quad (9)$$

where

$$a_n = \frac{2a_v \sin(n\pi a_1) \sin(n\pi a_v)}{n\pi a_1 n\pi a_v} \quad a_v = \frac{1.25T_r + T_w}{T_p} \quad a_1 = \frac{1.25T_r}{T_p} \quad \omega_n = \frac{2n\pi}{T_p} \quad (10a-d)$$

A symmetrical trapezoid provides a reasonable representation of a digital pulse and, unlike a square wave, has a finite rise time. This permits study of rise time dependent effects. In order to compare the results with the corresponding obtained by Bandler et al. [4], a rise time of 1.2 ns and a pulse width of 4.5 ns were chosen. Sixteen harmonics were used to represent the input signal. Figs. 12 and 13 shows the time domain circuit output voltages, V_a , V_b , V_c and V_d , as well as the input trapezoid signal. Once again, the higher crosstalk obtained is from V_a to V_b outputs.

Comparing the results shown in Fig. 12 with the results obtained by Bandler et al. [4] (see appendix B), the accuracy of the approach followed is acceptable, since the results agree more with the ones obtained using the electromagnetic simulators *em*TM and *IE3D*TM than those corresponding to Walker's formulas. This is more clearly shown in Fig. 14, in which the different simulation results were juxtaposed using the same physical scale for each plot. Notice that the frequency domain model waveforms were shifted to the left, because they correspond to a periodic input trapezoid signal that does not start at zero seconds.

VI. CROSSTALK MINIMIZATION

A. Problem formulation

For the circuit shown in Fig. 8, assuming that

- (a) all the lumped components values are fixed
- (b) ϵ_r and μ_r are fixed
- (c) w , h , ϵ_r and μ_r are the same for the three interconnects
- (d) w , h , d and l are the design parameters,

design the three interconnects so that the crosstalk from V_a to V_b is less than 0.02 (-34 dB) within an operating frequency range from 500MHz to 5 GHz, and the following constraints are satisfied:

$$0.25 \text{ mm} < w < 1 \text{ mm}$$

$$0.5 \text{ mm} < h < 2 \text{ mm}$$

$$0.5 \text{ mm} < d < 10 \text{ mm}$$

$$L_1 = 0.5 L_2$$

$$L_2 = L_3$$

$$2 \text{ cm} < L_2 < 20 \text{ cm}$$

B. Results

Before optimization, the simulation results obtained are shown in Fig. 15, using the following physical parameter values for the interconnect:

$$w = 0.7435 \text{ mm}, h = 1.5 \text{ mm}, d = 3.1925 \text{ mm}, L_2 = 5.5 \text{ cm}, \epsilon_r = 5.1825 \text{ and } \mu_r = 1$$

Running the optimization process using an l_1 optimizer, the crosstalk specification is satisfied as shown in Fig. 16. The following solution was found after 12 iterations that took 4 minutes and 38 seconds of CPU time, using *OSA90/hope*TM through a PC 486 connected in a Telnet session to a Sun Sparc station 10:

$$w = 0.7284 \text{ mm}, h = 0.5 \text{ mm}, d = 2.185 \text{ mm}, L_2 = 5.33 \text{ cm}$$

Finally, the time domain simulation of the crosstalk voltage using the same trapezoid signal described previously is illustrated in Fig. 17; the results before and after optimization are shown.

VII. CONCLUSIONS

A simple frequency domain approach to efficiently simulate and minimize the crosstalk between interconnects is proposed. For most practical circuits, the crosstalk between interconnects may vary extremely with frequency. Crosstalk minimization following a time domain-transient response approach does not guarantee that crosstalk specification will be fulfilled within the whole operating frequency range of the interconnects. The method proposed permits a straightforward crosstalk minimization in the

frequency range of interest, as well as time domain measurements by using the Harmonic Balance technique.

APPENDIX A: WALKER'S FORMULAS

The self inductance for each conductor and the ground plane is given by

$$L_s = \frac{\mu_r \mu_o}{K_{L1}} \left(\frac{h}{w} \right) - \frac{\mu_r \mu_o}{4\pi} \ln \left[1 + \left(\frac{2h}{d} \right)^2 \right] \quad \text{H/m} \quad (\text{A1})$$

The mutual inductance between the two conductors

$$L_m = \frac{\mu_r \mu_o}{4\pi} \ln \left[1 + \left(\frac{2h}{d} \right)^2 \right] \quad \text{H/m} \quad (\text{A2})$$

The capacitance between each conductor and the ground plane is

$$C_s = \varepsilon_r \varepsilon_o K_{C1} \left(\frac{w}{h} \right) \quad \text{F/m} \quad (\text{A3})$$

The capacitance between both conductors

$$C_m = \frac{\varepsilon_r \varepsilon_o}{4\pi} K_{C1} K_{L1} \left(\frac{w}{h} \right)^2 \ln \left[1 + \left(\frac{2h}{d} \right)^2 \right] \quad \text{F/m} \quad (\text{A4})$$

where the fringing factors are

$$K_{L1} = \frac{120\pi}{Z_{0(\varepsilon_r=1)}} \left(\frac{h}{w} \right) \quad (\text{dimensionless}) \quad (\text{A5})$$

$$K_{C1} = \left[\frac{120\pi}{Z_{0(\varepsilon_r=1)}} \left(\frac{h}{w} \right) \sqrt{\frac{\varepsilon_e}{K_{L1} \varepsilon_r}} \right]^2 \quad (\text{dimensionless}) \quad (\text{A6})$$

and the characteristic impedance of each channel is

$$Z_{0(\varepsilon_r=1)} = 60 \ln \left(\frac{8h}{w} + \frac{w}{4h} \right) \quad \Omega \quad \text{for} \quad \frac{w}{h} \leq 1 \quad (\text{A7})$$

$$Z_{0(\varepsilon_r=1)} = \frac{120\pi}{\left(\frac{w}{h} \right) + 2.42 - 0.44 \left(\frac{h}{w} \right) + \left(1 - \frac{h}{w} \right)^6} \quad \Omega \quad \text{for} \quad \frac{w}{h} \geq 1 \quad (\text{A8})$$

Some practical design considerations concerning Walker's formulas are presented below.

Effective dielectric constant

The effective dielectric constant, ϵ_e , accounts for nonhomogeneity of the region surrounding conductors.

As $2h/w$ approaches zero, the effective dielectric constant (ϵ_e) approaches the dielectric constant of the PWB laminate (ϵ_r), because most of the electric flux is totally in it. Conversely, as $2h/w$ becomes large, the effective dielectric constant approaches the average of the air (ϵ_o) and the laminate dielectric constants. In other words, the effective dielectric constant is the dielectric constant of a homogeneous medium that replaces the air and PWB laminate. Following Pozar [15]:

$$\epsilon_e = \frac{\epsilon_r + 1}{2} + \frac{\epsilon_r - 1}{2} \frac{1}{\sqrt{1 + 12h/w}} \quad (\text{A9})$$

Fringing factors

The fringing factor K_{C1} , takes into account the flux fringing of the electric field lines in a “parallel” plate capacitor. As the rate h/w increases, the actual capacitance increases, resulting a greater value than would be predicted from direct parallel plate equations, neglecting fringing. If the medium surrounding the flat conductor and the parallel plane were homogeneous, the capacitive fringing factor would be equal to the inductive one ($K_{C1} = K_{L1}$). However, in this case, the flat conductor is separated from the ground plane by the PBW laminate with relative dielectric constant, ϵ_r , and the region above the conductor is assumed to have a relative dielectric constant $\epsilon_r = 1$, so that the medium surrounding the conductor is not homogeneous.

Effects on crosstalk

A ground plane greatly reduces the mutual capacitance and mutual inductance and hence crosstalk between two conductors. The mutual capacitance is very distance sensitive. Decreasing the spacing d by a factor of x , increases the mutual capacitance by a factor x^2 . The mutual inductance per unit length has the same behavior. This is due to the fact that

$$\ln\left(1+\left(\frac{2h}{d}\right)^2\right)\approx\left(\frac{2h}{d}\right)^2 \quad \text{when } d \gg 2h \quad (\text{A10})$$

APPENDIX B: TRANSIENT RESPONSES OBTAINED BY BANDLER ET AL. [4]

Similar results were obtained for the line width and the substrate thickness. The largest discrepancy appears when varying the line width (see Fig. 3).

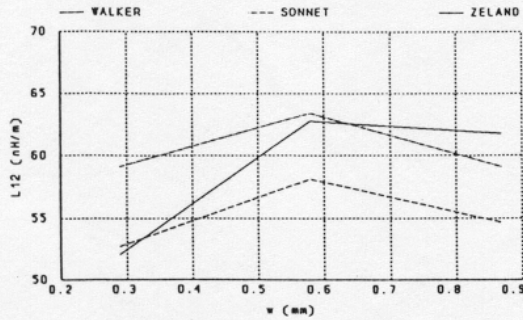


Fig. 3 L_{12} vs. the line width.

IV. CROSSTALK ANALYSIS

The differences between the LC matrices obtained by the three approaches considered can be better understood by comparing the responses of a more complex circuit embedding the coupled transmission lines as subcircuits.

We consider crosstalk analysis of the circuit shown in Fig. 4 (Lum, Nakhla and Zhang [11]).

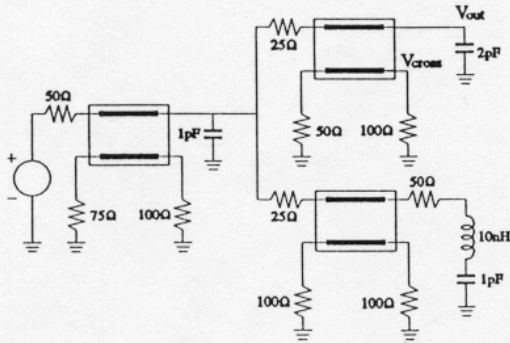


Fig. 4 The interconnect circuit for model comparison.

The LC matrices determined from the empirical formulas and from EM simulations are incorporated into the AWE time-domain circuit-level simulator COFFEE2 [5] developed at Carleton University. The simulator is driven by OSA90/hope through a Datapipe [7] connection. In this manner it is ready for optimization controlled by OSA90/hope.

Applying a 6 ns trapezoidal voltage shown in Fig. 5 to the circuit input we evaluate various responses.

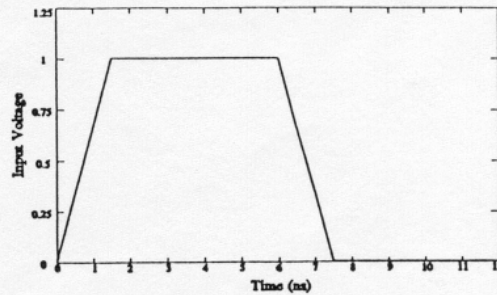


Fig. 5 Trapezoidal input signal.

Three voltage waveforms at the first output port corresponding to the three coupled-line models are shown in Fig. 6. They appear to be almost identical.

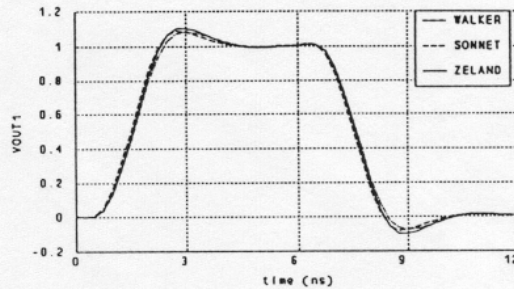


Fig. 6 Voltage waveforms at the first output port.

The corresponding crosstalk voltage waveforms at the first output port are shown in Fig. 7. In this case we can notice a larger difference between the results. The responses corresponding to both EM simulations are fairly consistent while the response generated by the empirical formulas differs from the other two by up to 50%.

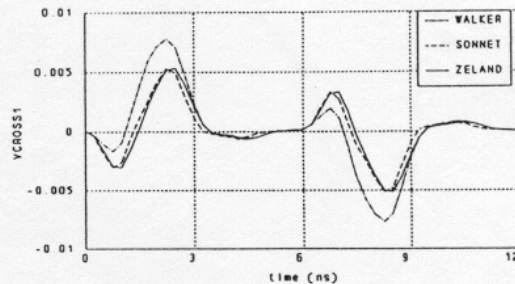


Fig. 7 Crosstalk waveforms at the first output port.

REFERENCES

- [1] D.S. Gao, A.T. Yang and S.M. Kang, "Modeling and simulation of interconnection delays and crosstalks in High-Speed Integrated Circuits," *IEEE Trans. Circuits Syst.*, vol. 37, 1990, pp. 1-8.
- [2] T. Dhaene and D. De Zutter, "Selection of lumped element models for coupled lossy transmission lines," *IEEE Trans. Computer-Aided Design*, vol. 11, 1992, pp. 805-815.
- [3] C.S. Walker, *Capacitance, Inductance and Crosstalk Analysis*. Norwood, MA: Artech House, 1990.
- [4] J.W. Bandler, R.M. Biernacki and S.H. Chen, "Toward direct EM optimization of VLSI interconnects: validation of coupled transmission line models," *Proc. 1995 Canadian Conf. Electrical and Computer Engineering* (Montreal, Canada), 1995, pp. 377-380.
- [5] V.K. Tripathi and J.B. Retting, "A SPICE model for multiple coupled microstrips and other transmission lines," *IEEE Trans. Microwave Theory Tech.*, vol. MTT-33, 1985, pp. 1513-1518.
- [6] M. Kirschning and R. Jansen, "Accurate wide-range design equations for the frequency-dependent characteristics of parallel coupled microstrip lines," *IEEE Trans. Microwave Theory Tech.*, vol. MTT-32, 1984, pp. 83-90. Corrections: *IEEE Trans. Microwave Theory Tech.*, vol. MTT-33, 1985, p. 288.
- [7] J.J. Choma, *Electrical Networks: Theory and Analysis*. New York: Wiley, 1985, pp. 523-526.
- [8] S. Lum, M.S. Nakhla and Q.J. Zhang, "Sensitivity analysis of lossy coupled transmission lines," *IEEE Trans. Microwave Theory Tech.*, vol. MTT-39, 1991, pp. 2089-2099.
- [9] *Design Center*TM, Microsim Corporation, 20 Fairbanks, Irvine, CA 92718, 1997.
- [10] *em*TM, Sonnet Software, Inc., 135 Old Cove Road, Suite 203, Liverpool, NY 13090-3774, 1994.
- [11] *IE3D*TM, Zeland Software, Inc., 3910 Mission Street, San Francisco, CA 94112, 1994.
- [12] E. Chiprout and M.S. Nakhla, *Asymptotic Wave Evaluation and Moment Matching for Interconnect Analysis*. Boston, MA: Kluwer, 1994.
- [13] *OSA90/hope*TM, Optimization Systems Associates Inc., Dundas, Ontario, Canada L9H 5E7, 1997.
- [14] R.A. Sainati and T.J. Moravec, "Estimating high speed circuit interconnect performance," *IEEE Trans. Circuits Syst.*, vol. 36, 1989, pp. 533-540.
- [15] M. Pozar, *Microwave Engineering*. Amherst, MA: John Wiley and Sons, 1998.

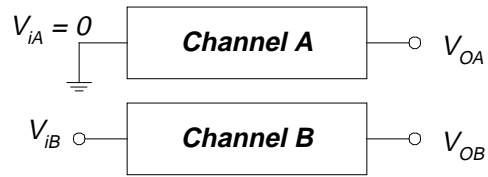


Fig. 1 Generic two channels system.

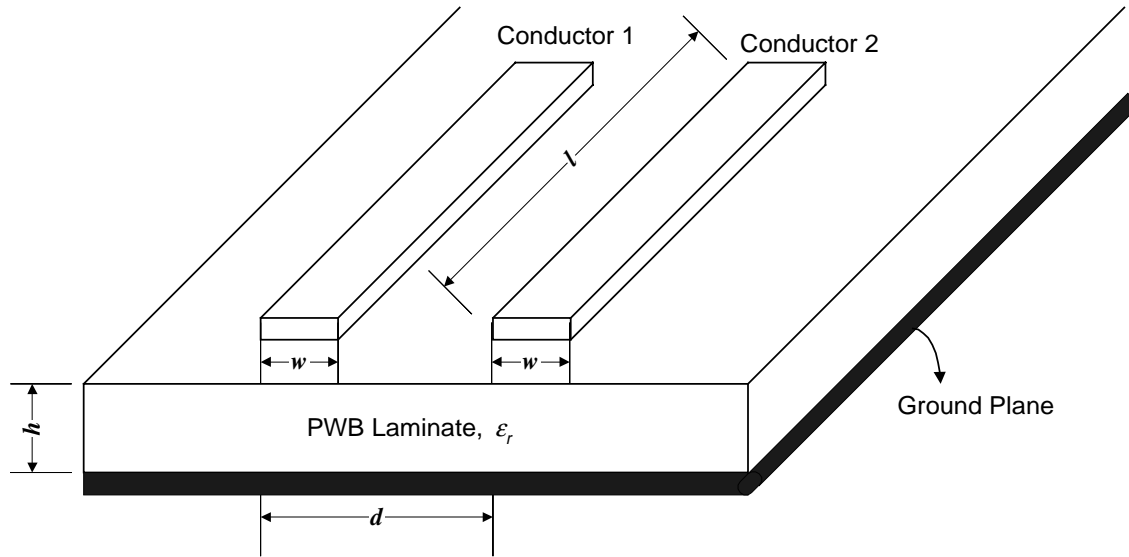


Fig. 2 Physical structure of a coupled microstrip interconnect.

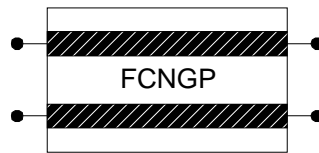


Fig. 3 Symbol of the coupled microstrip interconnect.

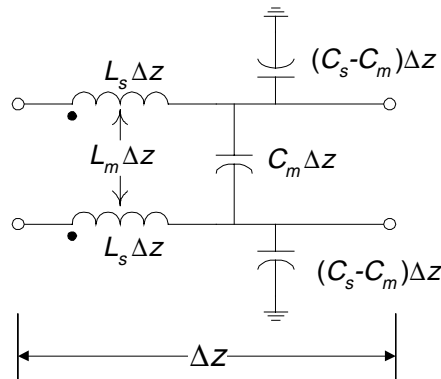


Fig. 4 Equivalent circuit of the coupled microstrip interconnect.

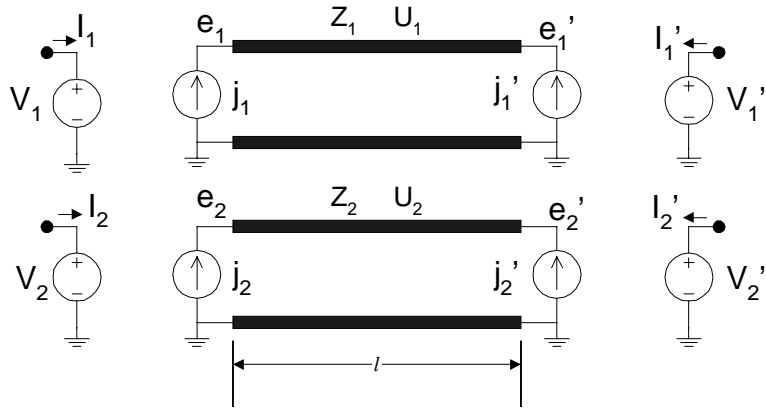


Fig. 5. A SPICE model for a coupled microstrip interconnect.

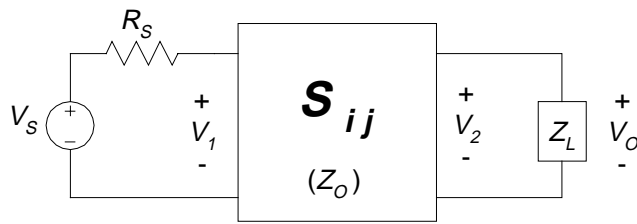


Fig. 6 General two port circuit.

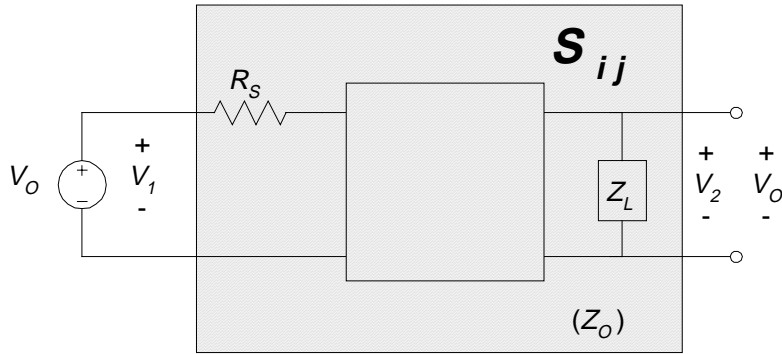


Fig. 7 General two port circuit, with network expanded.

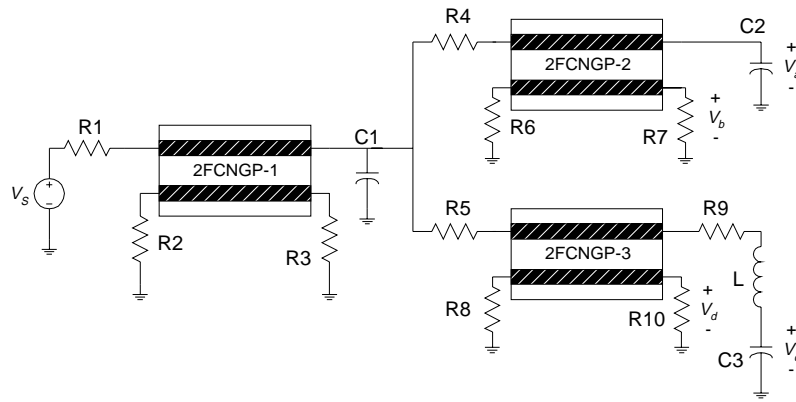


Fig. 8 Circuit to be simulated.

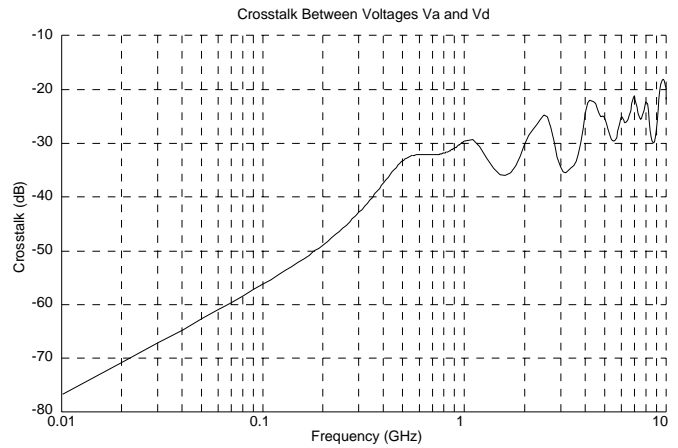
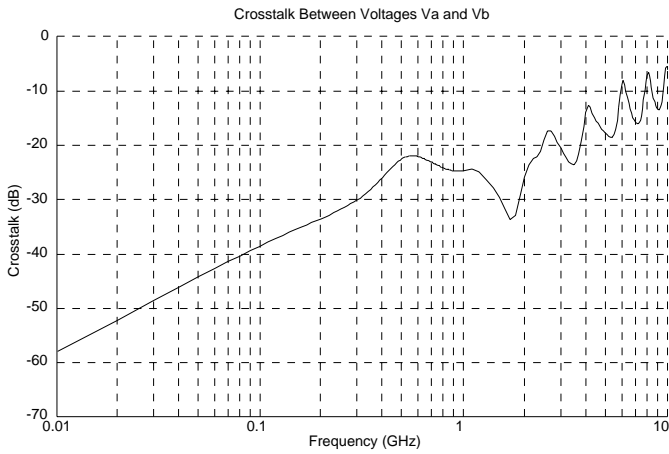


Fig. 9 Frequency domain results (crosstalk from output a to outputs b and d).

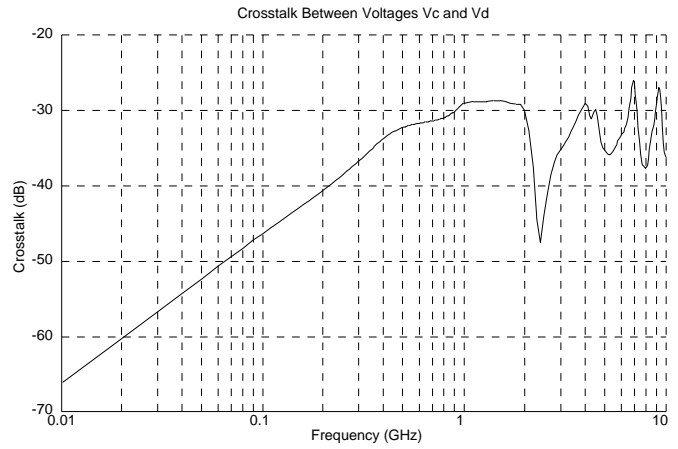
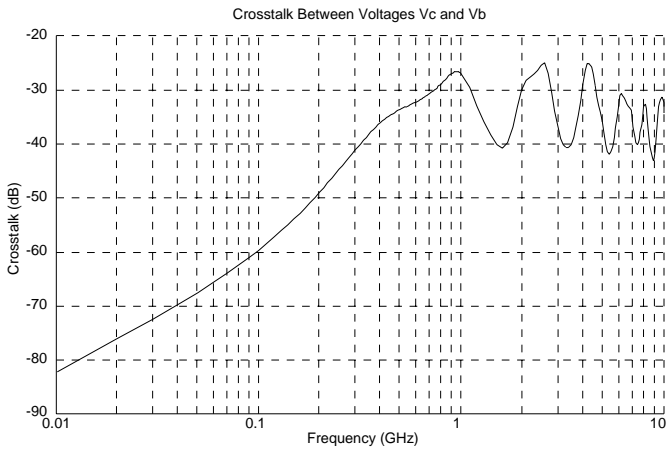


Fig. 10 Frequency domain results (crosstalk from output c to outputs b and d).

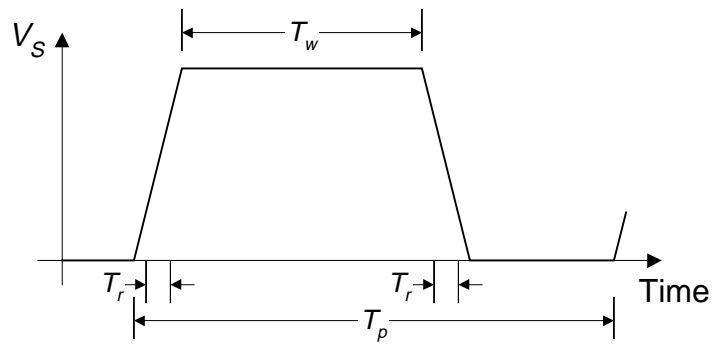


Fig. 11 Symmetrical trapezoid signal.

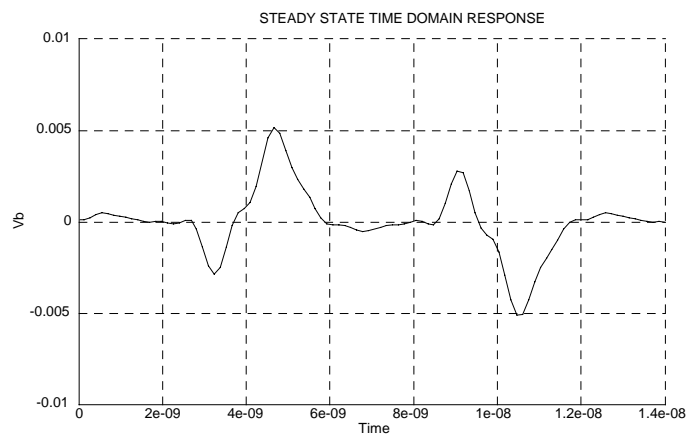
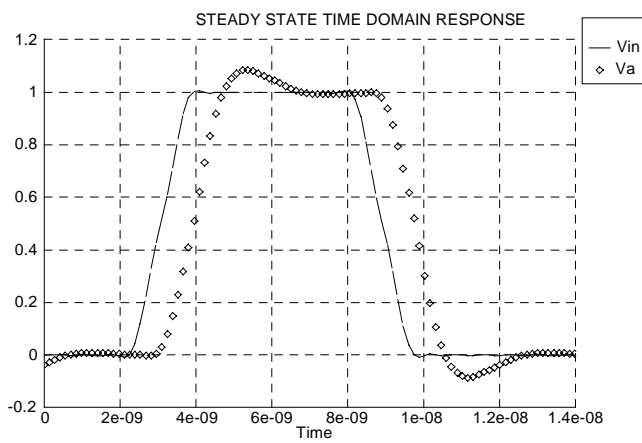


Fig. 12 Time domain results (output voltages V_a and V_b).

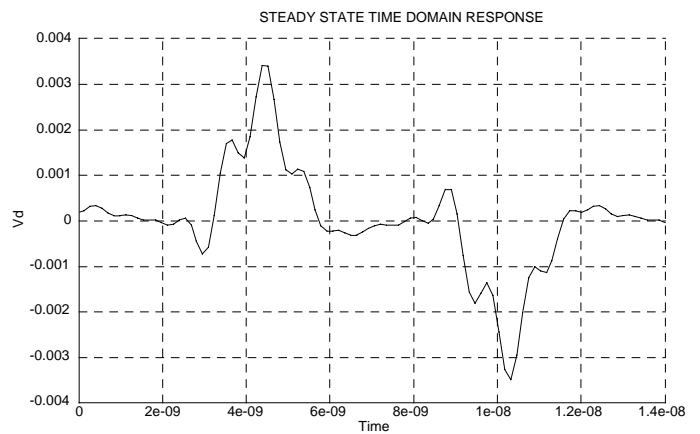
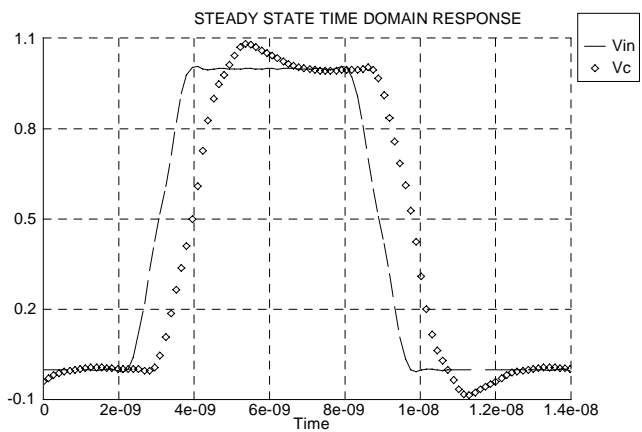
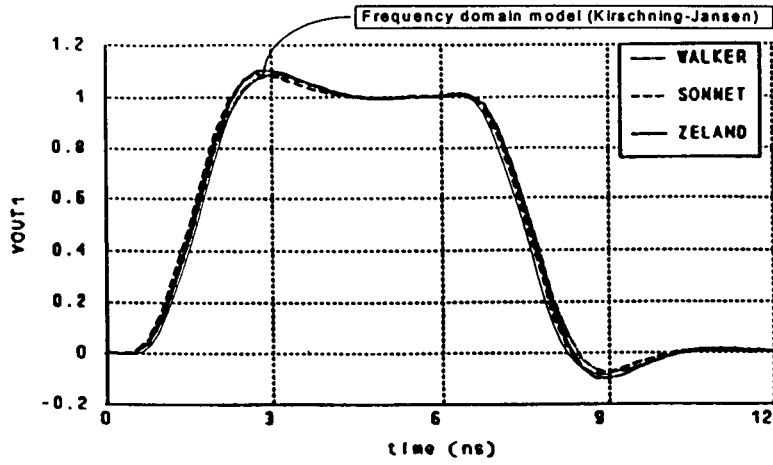
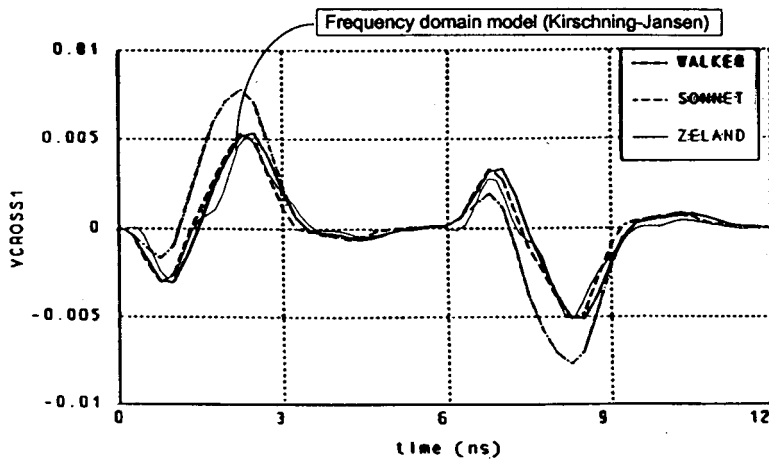


Fig. 13 Time domain results (output voltages V_c and V_d).



(a) Output voltage V_a (VOUT1)



(b) Output voltage V_b (VCROSS1)

Fig. 14 Direct comparison between simulation results using the following models: Walker's, Sonnet's, Zeland's and Kirschning-Jansen's.

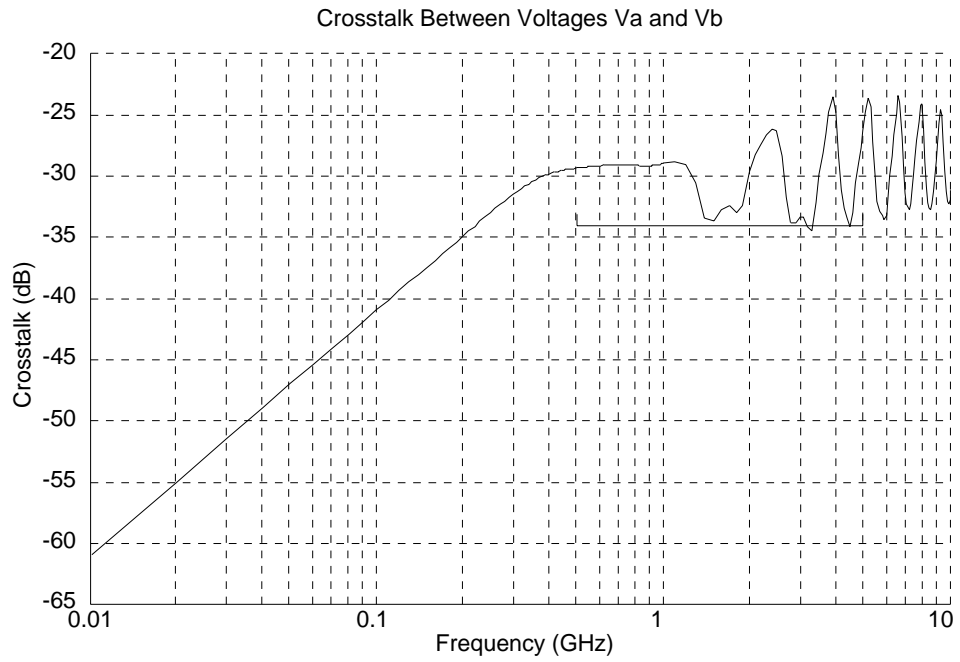


Fig. 15 Crosstalk before optimization.

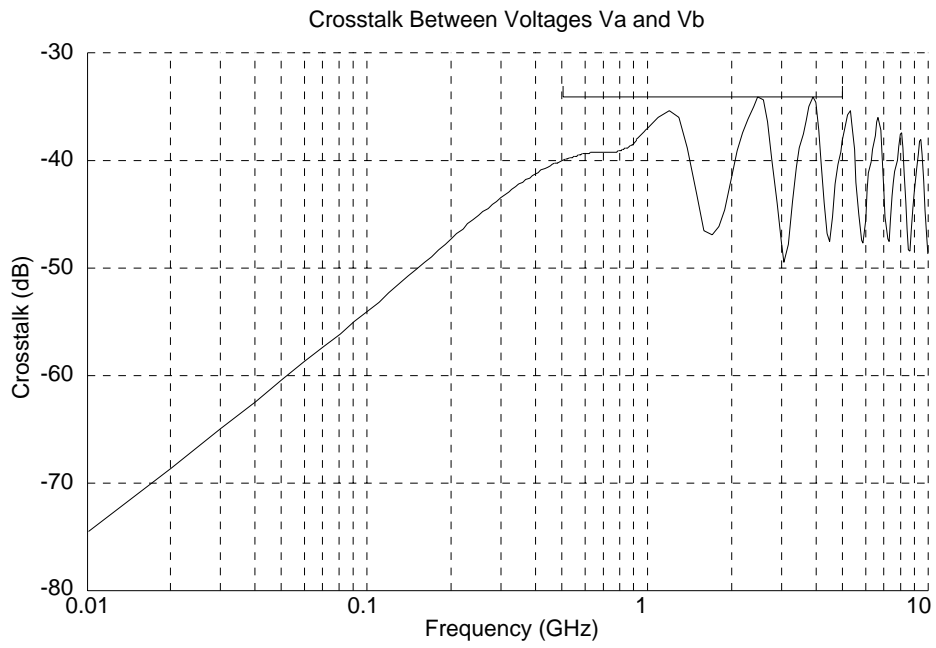
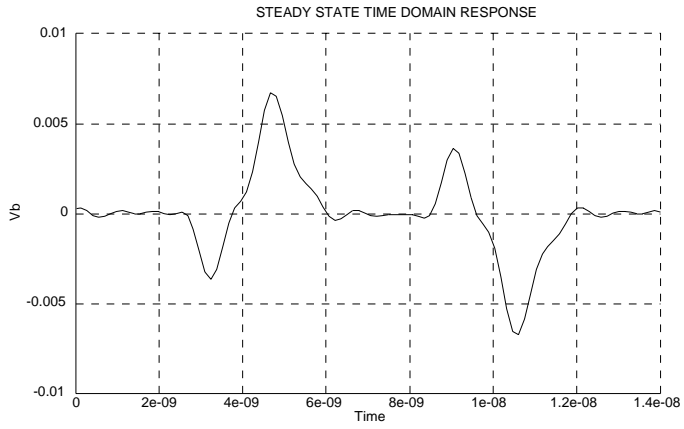
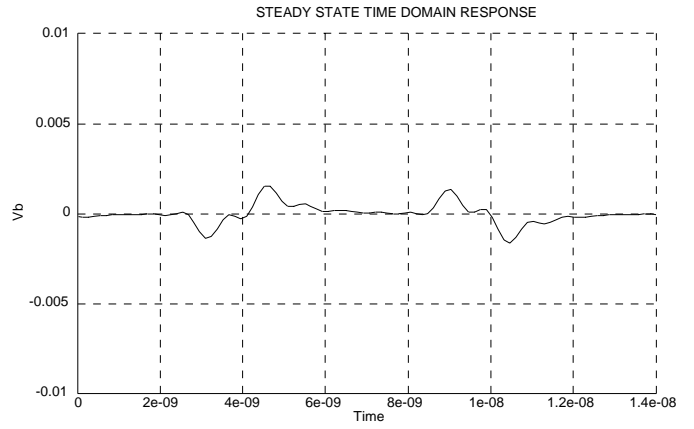


Fig. 16 Crosstalk after optimization.



a) Crosstalk voltage before optimization



b) Crosstalk voltage after optimization

Fig. 17 Time domain results.